# Large deformation and electromechanical instability of a dielectric elastomer tube actuator

Jian Zhu,[1] Hristiyan Stoyanov,[2] Guggi Kofod,[2] and Zhigang Suo[1,a)]
[1]*School of Engineering and Applied Sciences and Kavli Institute, Harvard University, Cambridge, Massachusetts 02138, USA*
[2]*Institute of Physics and Astronomy, Applied Condensed-Matter Physics, University of Potsdam, Karl-Liebknecht-Str. 24/25, 14476 Potsdam-Golm, Germany*

(Received 4 June 2010; accepted 14 August 2010; published online 13 October 2010)

This paper theoretically analyzes a dielectric elastomer tube actuator (DETA). Subject to a voltage difference between the inner and outer surfaces, the actuator reduces in thickness and expands in length, so that the same voltage will induce an even higher electric field. This positive feedback may cause the actuator to thin down drastically, resulting in electrical breakdown. We obtain an analytical solution of the actuator undergoing finite deformation when the elastomer obeys the neo-Hookean model. The critical strain of actuation is calculated in terms of various parameters of design. We also discuss the effect of the strain-stiffening on electromechanical behavior of DETAs by using the model of freely joined links. © *2010 American Institute of Physics*. [doi:10.1063/1.3490186]

## I. INTRODUCTION

Dielectric elastomer actuators have received much attention recently due to their light weight, high energy density, and large deformation. Applications include soft robots, adaptive optics, and programmable haptic surfaces.[1] As one of the configurations proposed by Pelrine *et al.*,[2,3] a dielectric elastomer tube actuator (DETA) can be prepared as a long, slender actuator (Fig. 1). Compared to other dielectric elastomer configurations (say, planar actuators), DETAs have very low inactive-to-active material ratio and are less bulky and more versatile for applications.[4–7] DETAs can be manufactured in well-established industrial processes, such as extrusion, multicomponent fiber manufacturing technologies, etc.[5,6]

Subject to a voltage, a dielectric elastomer reduces its thickness and expands its area. This electromechanical coupling was investigated for planar actuators and found to agree with the Maxwell stress.[8] The electromechanical coupling was recently shown to be explained also with a formulation based on free energy.[9] Unfortunately, this mechanism of actuation makes such actuators susceptible to electromechanical instability.[10–16] Electromechanical instability is understood as follows. As the voltage increases, the elastomer thins down, so that the same voltage will induce an even higher electric field. Depending upon the nonlinear hyperelastic properties of the material, this positive feedback may cause the elastomer to thin down drastically, resulting in electrical breakdown.[2,3,10–16]

The existing model of DETAs invoked the theory of infinitesimal deformation and evaluated the Maxwell stress by using the thickness of the undeformed elastomer.[7] Such a model is effective when the strain of actuation is small. In practice, however, a DETA is normally prestretched by a load before a voltage is applied, so that the actuator is rarely in a small strain condition. To describe a DETA subject to a high prestretch or performing near electromechanical instability, this paper studies a DETA undergoing finite deformation. Sec. II develops the equations of state for the DETA in an analytical form. Sec. III studies the electromechanical instability. Section IV discusses numerical results. Section V extends the analysis beyond the neo-Hookean model by adopting a material model that accounts for the effect of finite contour length of polymer chains.

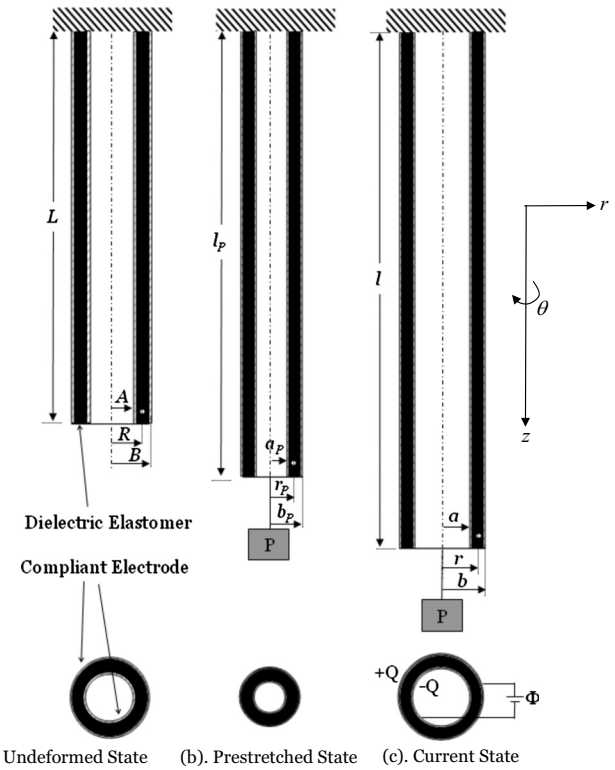


FIG. 1. Schematic of a tube of a dielectric elastomer coated with two compliant electrodes. (a) In the undeformed state, the tube is of length $L$, inner radius $A$, and outer radius $B$. (b) Prestretched by a load $P$, the tube is of length $l_p$, inner radius $a_p$, and outer radius $b_p$. (c) Subject to a load $P$ and a voltage $\Phi$, the tube is of length $l$, inner radius $a$, and outer radius $b$. The strain of actuation due to the voltage is defined as $(l-l_P)/l_P$.

a)Electronic mail: suo@seas.harvard.edu.

 

## II. EQUATIONS OF STATE

Figure 1 illustrates a tube of a dielectric elastomer, coated with compliant electrodes on both the inner and outer surfaces. When the tube is undeformed, the length is $L$, the inner radius is $A$, and the outer radius is $B$. When the tube is prestretched by an axial load $P$, the length is $l_P$, the inner radius is $a_P$, and the outer radius is $b_P$. The tube is then subject to a voltage difference $\Phi$ between the two inner and outer surfaces, causing a charge $Q$ on the inner surface, which is balanced by a charge on the outer one, and the tube deforms into a state of generalized plane strain, so that the axial strain takes the same value everywhere in the tube. In this state, the length is $l$, the inner radius is $a$, and the outer radius is $b$. A material particle of radius $R$ in the undeformed state moves to a place of radius $r$ in the current state.

The state of deformation of the tube is specified by the axial stretch $\lambda_z = l/L$ and the function $r(R)$. The elastomer is taken to be incompressible, so that the volume of the shell between radii $A$ and $R$ in the undeformed state equals that between radii $a$ and $r$ in the deformed state, namely,

$$(R^2 - A^2) = \lambda_z (r^2 - a^2). \tag{1}$$

Note that $A$ is fixed once the tube is fabricated. Consequently, the condition of incompressibility specifies the function $r(R)$ in terms of $\lambda_z$ and $a$. That is, we may regard the tube as a system of two degrees of freedom: $\lambda_z$ and $a$. In the deformed state, the outer radius is

$$b = \sqrt{a^2 + (B^2 - A^2)\lambda_z^{-1}}. \tag{2}$$

The hoop stretch is $\lambda_\theta = r/R$, and is expressed as a function of $r$

$$\lambda_\theta(r) = \frac{r}{\sqrt{A^2 + \lambda_z (r^2 - a^2)}}. \tag{3}$$

Due to incompressibility, the radial stretch is related to the axial and hoop stretches as $\lambda_r = (\lambda_z \lambda_\theta)^{-1}$. Thus,

$$\lambda_r(r) = \frac{\sqrt{A^2 + \lambda_z (r^2 - a^2)}}{r\lambda_z}. \tag{4}$$

In the deformed state, an element of the tube is in a state of triaxial stress: $\sigma_z$, $\sigma_r$, and $\sigma_\theta$. Mechanical equilibrium requires that

$$\frac{d\sigma_r}{dr} + \frac{\sigma_r - \sigma_\theta}{r} = 0. \tag{5}$$

Let $V(r)$ be the field of electric potential in the tube. The voltage applied between the inner and outer surfaces is $\Phi = V(b) - V(a)$. The electric field $E$ in the tube is in the radial direction, given by

$$E = -dV/dr. \tag{6}$$

Gauss's law requires that the electric displacement is divergence free, so that

$$D = \frac{Q}{2\pi r \lambda_z L}. \tag{7}$$

The material is assumed to be an ideal dielectric elastomer,[11] where the dielectric behavior of the elastomer is taken to be liquidlike, unaffected by deformation. This material model seems to describe some experimental data[17] but is inconsistent with other experimental data.[18] Nevertheless, this model has been used almost exclusively in previous analyses of dielectric elastomers and will be used in this paper. For a model of nonideal dielectric elastomers, see Ref. 19. For simplicity, we use neo-Hookean to illustrate the material nonlinearity; other nonlinear material models may be used.[20] Consequently, the material model is expressed by

$$\sigma_\theta - \sigma_r = \mu(\lambda_\theta^2 - \lambda_\theta^{-2}\lambda_z^{-2}) - \varepsilon E^2, \tag{8}$$

$$\sigma_z - \sigma_r = \mu(\lambda_z^2 - \lambda_\theta^{-2}\lambda_z^{-2}) - \varepsilon E^2, \tag{9}$$

$$D = \varepsilon E, \tag{10}$$

where $\varepsilon$ is the permittivity and $\mu$ the shear modulus.

The above equations govern the tube as a variable capacitor. In what follows, we express the axial force $P$ and voltage $\Phi$ in terms of $\lambda_z$ and $a$. A combination of Eqs. (6), (7), and (10) gives

$$\Phi = \frac{Q}{2\pi\varepsilon\lambda_z L}\log\frac{b}{a}. \tag{11}$$

This equation relates the voltage to the charge and various other parameters in Eq. (11). For the ideal dielectric elastomer, the dielectric behavior is liquidlike, so that the voltage-charge relation (11) depends on the parameters in the current state.

Inserting Eqs. (7), (8), and (10) into Eq. (5) and integrating $r$ from $a$ to $b$, we obtain that

$$Q = \sqrt{\mu\varepsilon}(2\pi LA)\sqrt{-1 + \lambda_z\left(\frac{a}{A}\right)^2 + \frac{2\lambda_z (a/A)^2}{1 - (a/b)^2}\log\frac{aB}{bA}}. \tag{12}$$

In evaluating the integral, we have used the boundary condition that both the inner and outer surfaces of the tube are traction free, $\sigma_r(a) = \sigma_r(b) = 0$. Substituting Eq. (2) and (12) into Eq. (11) yields

$$\Phi = \sqrt{\frac{\mu}{\varepsilon}\left(\frac{-A^2 + \lambda_z a^2}{\lambda_z^2} + \frac{2a^2b^2}{B^2 - A^2}\log\frac{aB}{bA}\right)}\log\frac{b}{a}. \tag{13}$$

Inserting Eqs. (7), (8), and (10) again into Eq. (5), but now integrating Eq. (5) from $a$ to $r$, we obtain the distribution of the radial stress

$$\sigma_r(r) = \frac{\mu}{\lambda_z}\left[\log\frac{aR}{Ar} - \frac{(r^2 - a^2)b^2}{(b^2 - a^2)r^2}\log\frac{aB}{bA}\right]. \tag{14}$$

Inserting Eq. (14) into Eqs. (8) and (9), we obtain that

$$\sigma_\theta(r) = \frac{\mu}{\lambda_z}\left[\log\frac{aR}{Ar} - \frac{(r^2 + a^2)b^2}{(b^2 - a^2)r^2}\log\frac{aB}{bA} + \frac{r^2\lambda_z}{R^2} - 1\right], \tag{15}$$

$$\sigma_z(r) = \frac{\mu}{\lambda_z}\left[\log\frac{aR}{Ar} - \frac{(r^2 + a^2)b^2}{(b^2 - a^2)r^2}\log\frac{aB}{bA} + \lambda_z^3 - 1\right]. \tag{16}$$

The axial force is given by

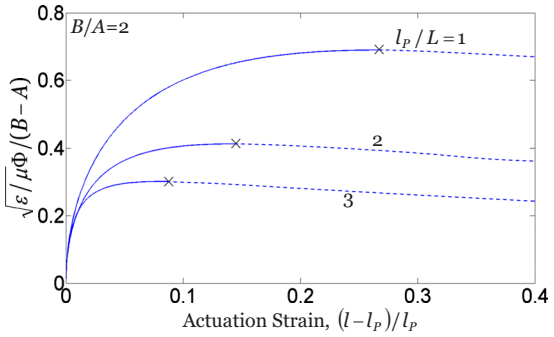


FIG. 2. (Color online) The voltage as a function of the strain of actuation at several levels of prestretch. When the voltage reaches a critical value, electromechanical instability occurs. The critical strain of actuation for the onset of the instability decreases as the prestretch increases.

$$P = \int_a^b 2\pi r \sigma_z(r) dr. \tag{17}$$

Substituting Eqs. (2) and (16) into Eq. (17) yields

$$P = \mu\pi\left[\left(\frac{A^2 - \lambda_z a^2}{\lambda_z^2}\right)\log\frac{B}{A} + \frac{(\lambda_z^3 - 1)(B^2 - A^2)}{\lambda_z^2} + \frac{2a^2b^2}{B^2 - A^2}\log\frac{Bb}{Aa}\log\frac{b}{a}\right]. \tag{18}$$

Equations (13) and (18) express $\Phi$ and $P$ in terms of $\lambda_z$ and $a$. Note that $b$ is expressed in terms of $\lambda_z$ and $a$ by Eq. (2).

In the absence of a voltage, $\Phi=0$, the axial force $P$ stretches the tube to the length $l_p$. In this prestretched state, the deformation in the tube is homogeneous, with $\lambda_z=l_p/L$, $\lambda_r=\lambda_\theta=\lambda_z^{-1/2}$, and $\sigma_r=0$. In addition, the axial force relates to the axial stress as $P=\sigma_z\pi(b^2-a^2)=\sigma_z\pi(B^2-A^2)/\lambda_z$. Using these relations and setting $E=0$ in Eq. (9), we obtain that

$$P = \pi\mu(B^2 - A^2)\left[\frac{l_p}{L} - \left(\frac{l_p}{L}\right)^{-2}\right]. \tag{19}$$

## III. ELECTROMECHANICAL INSTABILITY

We now use the above equations to simulate the processes illustrated in Fig. 1. For a given axial force $P$, Eq. (19) gives the length $l_p$ of the tube in the prestretched state [Fig. 1(b)]. When both the axial force $P$ and the voltage $\Phi$ are prescribed, the tube deforms to the state with inner radius $a$ and length $l$ [Fig. 1(c)], and Eqs. (13) and (18) constitute a set of nonlinear algebraic equations for $a$ and $\lambda_z=l/L$. By definition, the strain of actuation due to the voltage is $(l-l_P)/l_P$. This section plots the solutions to these nonlinear algebraic equations, and interprets the solutions.

Figure 2 plots the voltage as a function of the strain of actuation at several levels of prestretch. At each prestretch, the voltage first increases, reaches a peak, and then decreases. When the voltage is above the peak, the tube cannot reach a state of equilibrium. When the voltage is below the peak, corresponding to each value of the voltage are two states of equilibrium. We will analyze the stability of these two states of equilibrium, using a linear perturbation method.[21] As will be shown later, the states of equilibrium represented by the solid lines are stable, while those represented by the dashed lines are unstable. Consequently, the peaks represent the critical states for the onset of electromechanical instability.

With the given axial force $P^0$ and voltage $\Phi^0$, the corresponding inner radius $a^0$ and axial stretch $\lambda_z^0$ are determined by the nonlinear algebraic equations as described in the previous section. Here, these equations are noted as

$$\Phi^0 = \Phi(a^0, \lambda_z^0), \tag{20}$$

$$P^0 = P(a^0, \lambda_z^0), \tag{21}$$

where $\Phi(a,\lambda_z)$ and $P(a,\lambda_z)$ are two nonlinear functions.

For the given loads $P^0$ and $\Phi^0$, we examine if another state of equilibrium exists near the state of equilibrium characterized by $a^0$ and $\lambda_z^0$. When the state $(a^0,\lambda_z^0)$ is perturbed by infinitesimal deviations, $\Delta a$ and $\Delta\lambda_z$, the perturbed state is characterized by $a=a^0+\Delta a$, and $\lambda_z=\lambda_z^0+\Delta\lambda_z$. If the perturbed state is also a state of equilibrium, it should satisfy the equations of state, namely,

$$\Phi^0 = \Phi(a^0 + \Delta a, \lambda_z^0 + \Delta\lambda_z), \tag{22}$$

$$P^0 = P(a^0 + \Delta a, \lambda_z^0 + \Delta\lambda_z). \tag{23}$$

Expanding these equations into the Taylor series to the terms linear in the perturbations $\Delta a$ and $\Delta\lambda_z$, and using Eqs. (20) and (21), we obtain that

$$\begin{bmatrix} \frac{\partial\Phi}{\partial a} & \frac{\partial\Phi}{\partial\lambda_z} \\ \frac{\partial P}{\partial a} & \frac{\partial P}{\partial\lambda_z} \end{bmatrix} \begin{bmatrix} \Delta a \\ \Delta\lambda_z \end{bmatrix} = \begin{bmatrix} 0 \\ 0 \end{bmatrix}. \tag{24}$$

The partial derivatives of the functions $\Phi(a,\lambda_z)$ and $P(a,\lambda_z)$ in Eq. (24) are evaluated at the state of equilibrium $(a^0,\lambda_z^0)$.

Equation (24) is an eigenvalue problem for $\Delta a$ and $\Delta\lambda_z$. The matrix in Eq. (24) is known as the Hessian. When the determinant of the Hessian vanishes, Eq. (24) has nontrivial solutions, so that electromechanical instability occurs, and the state of equilibrium is unstable. If the Hessian is positive definite, the free energy attains a local minimum at the state of equilibrium $(a^0,\lambda_z^0)$, so that this state of equilibrium is stable. When the Hessian has both positive and negative eigenvalues, the state of equilibrium $(a^0,\lambda_z^0)$ is a saddle point for the free energy and is unstable. Figure 3 plots the voltage and the determinant of the Hessian as functions of the strain of actuation. Observe that the peak of the voltage corresponds to the critical state for electromechanical instability, at which the determinant of the Hessian vanishes.

## IV. NUMERICAL RESULTS AND DISCUSSIONS

Figure 4 plots the critical strain of actuation as a function of the prestretch at several levels of $B/A$. When $B/A$ is fixed, the critical strain of actuation decreases with the prestretch. In other words, the prestretch applied in the axial direction cannot improve the critical axial strain of actuation. This observation is similar to that for a planar dielectric elastomer actuator. As shown in Figs. 3(c) and 3(d) of Ref. 12, when a planar actuator is uniaxially prestressed, the prestretch in one

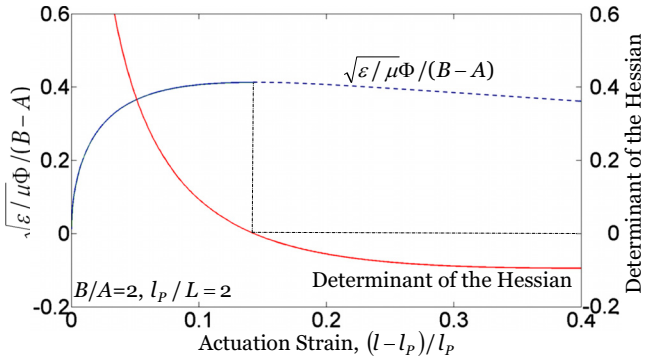


FIG. 3. (Color online) Electromechanical instability occurs when the determinant of the Hessian vanishes.

direction can decrease the critical strain of actuation in the same direction, but improve the critical strain of actuation in the normal direction. The phenomena were also observed in the experiments.[3,17] Our present analysis also shows that the axial prestretch can improve the radial actuation of a DETA, which is ignored here since the controlled axial actuation can be more readily coupled into mechatronic systems, and thus is the main focus in the literature.[4–7] Arora *et al.*[6] did experiments to measure the axial strain of actuation of DETAs with different axial prestretches. First, they determined the breakdown voltages for all the prototypes, and then measured the strain of actuation as a function of the electric field. For a silicone prototype of DETA, when the axial prestretch is 150%, 200%, or 300%, the maximum axial strain of actuation is 7%, 5%, or 2%, respectively. These experimental observations are qualitatively consistent with our theoretical predictions.

Figure 4 also shows that the critical strain of actuation increases with $B/A$ when the prestretch is fixed. For example, when $l_P/L=2$, the critical axial strain is 14%, 18%, 24%, or 28% for $B/A=2$, 10, 100, or 1000, respectively. For the DETAs with the same inner radius $A$, we can increase the critical strain of actuation by increasing the thickness and outer radius $B$. For the DETAs with the same thickness, we can increase the critical strain of actuation by decreasing the inner radius $A$ (thus increasing $B/A$). In the limit $B/A\to 1$,

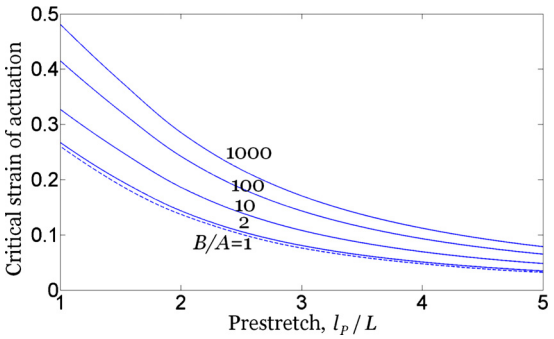


FIG. 4. (Color online) The critical strain of actuation as a function of the prestretch at several levels of $B/A$. The critical strain of actuation decreases as the prestretch increases but increases as $B/A$ increases. In the limit $B/A\to 1$, the DETA behaves exactly like a planar dielectric elastomer actuator.

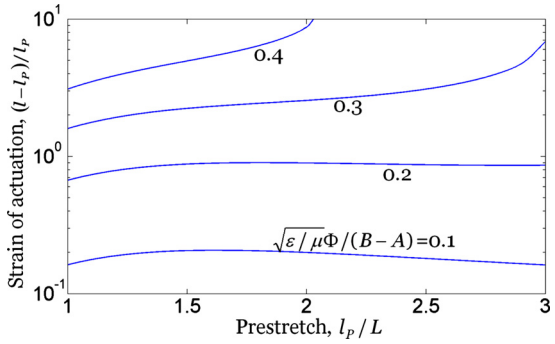


FIG. 5. (Color online) The strain of actuation as a function of the prestretch at several values of voltage. The tube has $B/A=2$.

the DETA behaves exactly like a planar dielectric elastomer actuator, which has been extensively studied in the literature.[8,10–16]

Figure 5 plots the strain of actuation as a function of the prestretch at several values of voltage. At a low and fixed voltage, an optimal prestretch can induce the largest strain of actuation. For example, when the voltage is fixed as $\sqrt{\varepsilon/\mu}\Phi/(B-A)=0.1$, the largest strain of actuation is attained when the prestretch is $l_p/L\approx 1.6$. At a high and fixed voltage, however, the strain of actuation increases with the prestretch. The phenomenon of the optimal prestretch with a small strain less than 2% is also observed in the experiment.[4]

## V. EFFECT OF STRAIN-STIFFENING OF ELASTOMERS

The available experimental data for DETAs are limited to small strains of actuation. Such experimental explorations may be aided by the neo-Hookean model presented in Sec. II. However, dielectric elastomers used in practice may exhibit strain-stiffening due to the finite contour length of polymer chains. This phenomenon cannot be described by a neo-Hookean model. In what follows, we illustrate electromechanical behavior of a DETA with an Arruda–Boyce material.[22]

The Arruda–Boyce model represents the molecule by a freely jointed chain of links[20] and represents an elastomer by a unit cell of eight chains.[22] The stretch of the polymer chain is related to the stretches of the elastomer as

$$\Lambda=\sqrt{\frac{\lambda_1^2+\lambda_2^2+\lambda_3^2}{3}}, \tag{25}$$

where $\Lambda$ is the stretch of each polymer chain, and $\lambda_1$, $\lambda_2$, and $\lambda_3$ are the principal stretches of the elastomer. The force-stretch behavior of the polymer chain is described by

$$\Lambda=\sqrt{n}\left(\frac{1}{\tanh\zeta}-\frac{1}{\zeta}\right), \tag{26}$$

where $n$ is the number of links per polymer chain and $\zeta$ the normalized force in the polymer chain. The free energy per unit volume of the elastomer is given by

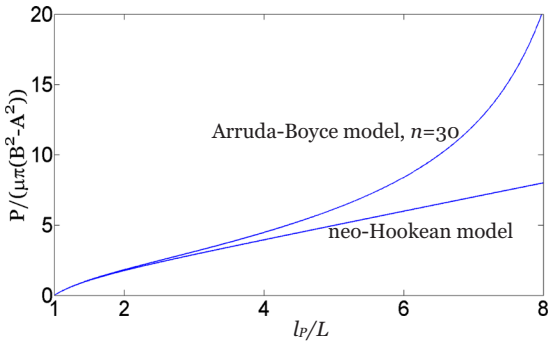


FIG. 6. (Color online) Force-displacement curves for the neo-Hookean model and the Arruda–Boyce model.

$$W = \mu n\left(\frac{\zeta}{\tanh\zeta} - 1 + \log\frac{\zeta}{\sinh\zeta}\right), \tag{27}$$

where $\mu$ is the shear modulus. The DETA with an Arruda–Boyce material can still be studied by using the method described in Sec. II. For example, Eqs. (1)–(7), (10), (11), and (17) are still applicable. However, we cannot obtain analytical expressions for Eqs. (12)–(16) and (18).

When the tube is prestretched by a load $P$ as shown in Fig. 1(b), Eq. (19) becomes

$$P = \pi\mu(B^2 - A^2)\frac{\sqrt{n}\xi}{3\Lambda}\left[\frac{l_p}{L} - \left(\frac{l_p}{L}\right)^{-2}\right]. \tag{28}$$

Figure 6 plots the normalized force as a function of the stretch. For the Arruda–Boyce material with $n=30$, the tube exhibits strain-stiffening when the stretch is large (say, when $l_P/L=6$). In addition, it should be noted that the Arruda–Boyce model recovers the neo-Hookean model when $n\to\infty$.

When the tube is subject to a voltage $\Phi$ as shown in Fig. 1(c), Eqs. (8) and (9) become

$$\sigma_\theta - \sigma_r = \frac{\mu\sqrt{n}\xi(\lambda_\theta^2 - \lambda_\theta^{-2}\lambda_z^{-2})}{3\Lambda} - \varepsilon E^2, \tag{29}$$

$$\sigma_z - \sigma_r = \frac{\mu\sqrt{n}\xi(\lambda_z^2 - \lambda_\theta^{-2}\lambda_z^{-2})}{3\Lambda} - \varepsilon E^2. \tag{30}$$

Following the method described in Sec. II, we plot the voltage as a function of the strain of actuation, as show in Fig. 7.

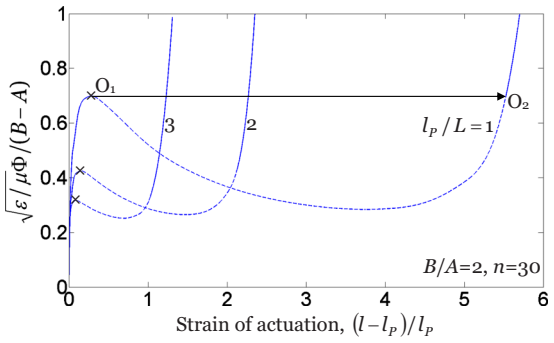


FIG. 7. (Color online) The voltage as a function of the strain of actuation at several levels of prestretch for a DETA with an Arruda–Boyce material. The DETA undergoes snap-through instability when the voltage reaches the peak.

The electromechanical behavior is interpreted as follows. For example, for the case with $l_P/L=1$, as the stretch increases, the voltage rises, reaches a peak and falls, because the same voltage gives higher electric field when the tube thins. After falling, the voltage rises again, because the polymer chains approach the limiting stretches, and the elastomer exhibits the strain-stiffening. In addition, if the tube is subject to a ramping voltage, the tube may undergo snap-through instability, jumping from $O_1$ to $O_2$, and the states represented by the dashed line are unreachable.

Zhao and Suo distinguish three types of dielectrics according to where electrical breakdown occurs.[23] A type I dielectric suffers electrical breakdown prior to electromechanical instability, and is capable of a small deformation of actuation. A type II dielectric reaches the peak, suffers electromechanical instability, and thins down excessively, leading to electrical breakdown. The deformation of actuation is limited by the stretch at which the voltage reaches the peak. A type III dielectric survives snap-through instability, reaches a stable state before electrical breakdown, and attains a large deformation of actuation. The strain-stiffening of elastomers may have little effect on the typed I and II DETAs, however, plays an important role in the type III DETA. For dielectric elastomers, how to survive snap-through instability and achieve a larger deformation of actuation is an interesting and important issue and deserves further studies.[23,24]

## VI. CONCLUDING REMARKS

This paper investigates a DETA, prestretched by a load and actuated by a voltage. We developed an analytical solution for the DETA undergoing finite deformation. When the voltage is less than a critical value, the actuator reaches a state of equilibrium. We analyze the instability of states of equilibrium, using a linear perturbation method, and further study the effects of the prestretch and the geometry parameter on electromechanical instability. We show that the critical strain of actuation increases as the ratio of the outer radius to the inner radius increases but decrease as the prestretch increases. We discuss the effect of the strain-stiffening on electromechanical behavior of DETAs. It is hoped that experimental data will be made available to be compared with the predictions of the theory.

## ACKNOWLEDGMENTS

This work is supported by NSF through a grant on Soft Active Materials (Grant No. CMMI-0800161), and by DARPA through a contract on Programmable Matter (Grant No. W911NF-08-1-0143). Z.G.S. acknowledges the support of the Kavli Institute at Harvard University. J.Z. thanks the Canadian Government for a postdoctoral fellowship. G.K. and H.S. acknowledge support from the WING initiative of the Germany Ministry of Education and Research through its NanoFutur Program (Grant No. NMP/03X5511).

[1] F. Carpi, D. De Rossi, R. Kornbluh, R. Pelrine, and P. Sommer-Larsen, *Dielectric Elastomers as Electromechanical Transducers* (Elsevier, Oxford, 2008).
[2] R. Pelrine, R. D. Kornbluh, and J. P. Joseph, Sens. Actuators, A **64**, 77

(1998).
[3]R. Pelrine, R. Kornbluh, Q. B. Pei, and J. Joseph, Science **287**, 836 (2000).
[4]H. Stoyanov, G. Kofod, and R. Gerhard, Adv. Sci. Technol. (Faenza, Italy) **61**, 81 (2008).
[5]C. G. Cameron, J. P. Szabo, S. Johnstone, J. Massey, and J. Leidner, Sens. Actuators, A **147**, 286 (2008).
[6]S. Arora, T. Ghosh, and J. Muth, Sens. Actuators, A **136**, 321 (2007).
[7]F. Carpi and D. D. Rossi, Mater. Sci. Eng., C **24**, 555 (2004).
[8]G. Kofod and P. Sommer-Larsen, Sens. Actuators, A **122**, 273 (2005).
[9]Z. G. Suo, X. H. Zhao, and W. H. Greene, J. Mech. Phys. Solids **56**, 467 (2008).
[10]K. H. Stark and C. G. Garton, Nature (London) **176**, 1225 (1955).
[11]X. H. Zhao, W. Hong, and Z. G. Suo, Phys. Rev. B **76**, 134113 (2007).
[12]X. H. Zhao and Z. G. Suo, Appl. Phys. Lett. **91**, 061921 (2007).
[13]A. N. Norris, Appl. Phys. Lett. **92**, 026101 (2008).
[14]R. Díaz-Calleja, E. Riande, and M. J. Sanchis, Appl. Phys. Lett. **93**, 101902 (2008).
[15]Y. J. Liu, L. W. Liu, Z. Zhang, L. Shi, and J. S. Leng, Appl. Phys. Lett. **93**, 106101 (2008).
[16]M. Kollosche and G. Kofod, Appl. Phys. Lett. **96**, 071904 (2010).
[17]G. Kofod, P. Sommer-Larsen, R. Kronbluh, and R. Pelrine, J. Intell. Mater. Syst. Struct. **14**, 787 (2003).
[18]M. Wissler and E. Mazza, Sens. Actuators, A **138**, 384 (2007).
[19]X. H. Zhao and Z. G. Suo, J. Appl. Phys. **104**, 123530 (2008).
[20]L. R. G. Treloar, *The Physics of Rubber Elasticity* (Clarendon, Oxford, 1975).
[21]A. Chajes, *Principles of Structural Stability Theory* (Prentice-Hall, Englewood Cliffs, NJ, 1974).
[22]E. M. Arruda and M. C. Boyce, J. Mech. Phys. Solids **41**, 389 (1993).
[23]X. H. Zhao and Z. G. Suo, Phys. Rev. Lett. **104**, 178302 (2010).
[24]Z. G. Suo and J. Zhu, Appl. Phys. Lett. **95**, 232909 (2009).